The peeling strength analysis of sandwich structure with cohesive element model

Xishu Wang, *Yuhang* An, *Nannan* Dou, and *Zhengbin* Wu*

Tianjin Chinese Academy of Sciences Institute of Advanced Technology, No.3 Haitai-Development Six Road, Xiqing District, Tianjin, PR China

Abstract. In this study, cohesive element models are applied to the strength analysis of the sandwich structure. As the sandwich structures have been used increasingly in the field of automotive light-weighting, the strength analysis of the sandwich structures becomes an important research topic. Cohesive Zone Models (CZMs) can be used to predict the initiation and propagation of the material cracks. Therefore, the peeling strength of the sandwich structure is calculated and analyzed by the traction-separation law with various CZMs. Experiments have been performed to verify the effectiveness of the sandwich structure via cohesive element models analyzation.

Keywords: Cohesive element, Glass fiber composite, Aramid honeycomb, Simulation analysis.

1 Introduction

A lightweight structure can be optimized via the computer simulation experments[1] with the aid of practical experiences, where different lightweight structures can be obtained from new materials with fast speed and delivering unusual organic shaped designs.[2]

As the name implies, honeycomb material resembles the structure of beehives which is a unique material as an excellent solution for various aerospace applications. Honeycomb material has been commonly used in the center of the sandwich-structure composites, i.e. the central layer between two thin panels.3 Such sandwich form can effectively combine the light-weight and high-strength qualities of the honeycomb which is essential in the aerospace industry with smooth and flat surfaces of the panels for easy installation. The panels can eliminate openings and unwanted airflow. Honeycomb material can be designed and manufactured with any number of cell shapes, sizes and configurations, 4 processed with high flexibility and high strength.

The carbon-fiber reinforced materials with the honeycomb structure have made the light-weight structure a breakthrough.5 However, the mechanical performance of the entire physical structure is far more satisfying requiring more time consumption and more financial resources but less optimal structure. Hence, it is necessary to use more accurate computing system to simulate the strength and performance of the light-weight structures.

* Corresponding author: zb.wu@siat.ac.cn

Cohesive zone models (CZMs) have widely been used in structure analyzation, such as crack propagation, adhesive strength, material fracture properties. The concept of the cohesive fracture was proposed by Barenblatt where the opposite surfaces are assumed to be connected together by cohesive forces in a narrow region ahead of the crack tip.6 the inelastic zone in front of the macro-crack can be modeled with a traction-separation relationship. Therefore, when two portions with cracks start to separate, there is traction in the separation region, and the magnitude of the traction is related to the characteristics of the material. The relationship details between the traction and separation can refer.7 to be specific, Daniel and Glaucio8 studied the CZMs in ABAQUS and proposed a library for further application exploration where ABAQUS can be used to analyze the traction-separation relationship of the model at the microscopic level. A finite element based on CZMs has been proposed to analyze the effect of humid environment on viscous degradation in ABAQUS, 9 in which various traction-separation relationships are summarized.

This study applies CZMs for the strength analysis of the honeycomb sandwich structures. The traction-separation laws in CZMs are used to study the strength of the sandwich structure composed of carbon fiber board and aluminum honeycomb during the load-bearing process, when the board and the honeycomb fall off. The mechanical model is constructed in the commercial finite element software for simulation analysis.

The remainder of the paper is organized as follows. Section Ⅱ discusses the CZMs in detail. The sandwich structure mechanic model is explained in Section Ⅲ, along with the experiments and result analysis. Conclusion is given in Section IV.

2 The review of CZMs

The exponential model, trapezoidal model and bilinear model are the most widely adopted CZMs,[10] which are explained for peel strength simulation.

2.1 Exponential CZM

The constitutive relation between the cohesive traction and the displacement jump can be written as,

$$T_n = -\frac{\phi_n}{\delta_{n1}}\exp(-\frac{\Delta_n}{\delta_n})\{\frac{\Delta_n}{\delta_n}\exp(-\frac{\Delta_\tau^2}{\delta_{\tau 1}^2})+\frac{1-q}{r-1}[1-\exp(-\frac{\Delta_\tau^2}{\delta_{\tau 1}^2})](r-\frac{\Delta_n}{\delta_{n1}})\} \tag{1}$$

$$T_\tau = -\frac{\phi_n}{\delta_{n1}}(2\frac{\delta_{n1}}{\Delta_{\tau 1}})\frac{\Delta_n}{\delta_{\tau 1}}\{q+(\frac{r-q}{r-1})\frac{\Delta_n}{\delta_{n1}}\}\exp(-\frac{\Delta_n}{\delta_{n1}})\exp(-\frac{\Delta_\tau^2}{\delta_{\tau 1}^2}) \tag{2}$$

Where $q=\phi_\tau/\phi_n$, $r=\Delta_n^*/\delta_{n1}$; ϕ_n and ϕ_τ are the normal and tangential separation, respectively; Δ_n and Δ_τ are the normal and tangential displacement jumps, respectively; δ_{n1} and $\delta_{\tau 1}$ are the normal and tangential interface characteristic lengths respectively; Δ_n^* is the value of Δ_n after complete shear separation occurs under the condition of normal traction vanishing. The normal and shear separations are related to the peak normal traction $\sigma_{\max}$ and the peak tangential traction $\tau_{\max}$, written as,

$$\phi_n = \sigma_{\max}\delta_{n1}\exp(1) \tag{3}$$

$$\phi_\tau = \sqrt{\exp(1)/2}\tau_{\max}\delta_{\tau 1} \tag{4}$$

2.2 Bilinear CZM

The cohesive constitutive relations for the bilinear CZM are given as,

$$T_n = \begin{cases} \dfrac{\sigma_{\max}}{\sigma_{n1}}\Delta_n & (\Delta_n \le \delta_{n1}) \\ \sigma_{\max}\dfrac{\delta_{\mathrm{n}}^f - \Delta_n}{\delta_{\mathrm{n}}^f - \delta_{n1}} & (\Delta_n > \delta_{n1}) \end{cases} \tag{5}$$

$$T_\tau = \begin{cases} \dfrac{\tau_{\max}}{\delta_{\tau 1}}\Delta_n & (\Delta_\tau \le \delta_{\tau 1}) \\ \tau_{\max}\dfrac{\delta_\tau^f - \Delta_\tau}{\delta_\tau^f - \delta_{\tau 1}} & (\Delta_\tau > \delta_{\tau 1}) \end{cases} \tag{6}$$

Where $\sigma_{\max}$ and $\tau_{\max}$ are the normal interface strength and tangential strength, respectively; δ_{n}^f and $\delta_{\tau 1}$ are the normal and tangential separations when the normal interface strength or tangential strength reaches its peak value; δ_{n}^f and δ_τ^f are the normal and tangential separations when complete separation occurs. The normal and tangential interface separations are given as,

$$\phi_n = \frac{1}{2}\sigma_{\max}\delta_n^f \tag{7}$$

$$\phi_\tau = \frac{1}{2}\tau_{\max}\delta_\tau^f \tag{8}$$

2.3. Trapezoidal CZM

The analytical expression of the trapezoidal CZM are given as,

$$T_n = \begin{cases} \dfrac{\sigma_{\max}}{\sigma_{n1}}\Delta_n & (\Delta_n \le \delta_{n1}) \\ \sigma_{\max} & (\delta_{n1} \le \Delta_n \le \delta_{n2}) \\ \dfrac{\sigma_{\max}}{\delta_{\mathrm{n}}^f - \delta_{n2}} \rightleftarrows (\delta_{\mathrm{n}}^f - \Delta_n) & (\delta_{n2} \le \Delta_n \le \delta_{\mathrm{n}}^f) \\ 0 & (\Delta_n > \delta_{\mathrm{n}}^f) \end{cases} \tag{9}$$

$$T_\tau = \begin{cases} \dfrac{\tau_{\max}}{\sigma_{\tau 1}}\Delta_\tau & (\Delta_\tau \le \delta_{\tau 1}) \\ \tau_{\max} & (\delta_{\tau 1} \le \Delta_\tau \le \delta_{\tau 2}) \\ \dfrac{\tau_{\max}}{\delta_\tau^f - \delta_{\tau 2}} \rightleftarrows (\delta_\tau^f - \Delta_\tau) & (\delta_{\tau 2} \le \Delta_\tau \le \delta_\tau^f) \\ 0 & (\Delta_\tau > \delta_\tau^f) \end{cases} \tag{10}$$

Where $\sigma_{\max}$ and $\tau_{\max}$ are the peak and normal shear traction for full normal and shear separation, respectively. δ_{n2}, δ_{n1}, δ_{n}^f, $\delta_{\tau 1}$, $\delta_{\tau 2}$ and δ_τ^f are the shape factors of the trapezoidal model for normal and shear tractions. The normal and tangential interface separations are written as,

$$\phi_n = \frac{1}{2}\sigma_{\max}(\delta_{n2} - \delta_{n1} + \delta_{\mathrm{n}}^f) \tag{11}$$

$$\phi_\tau = \frac{1}{2}\tau_{\max}(\delta_{\tau 2} - \delta_{\tau 1} + \delta_\tau^f) \tag{12}$$

The traction-separation relation of the three CZMs is illustrated in Fig.1.

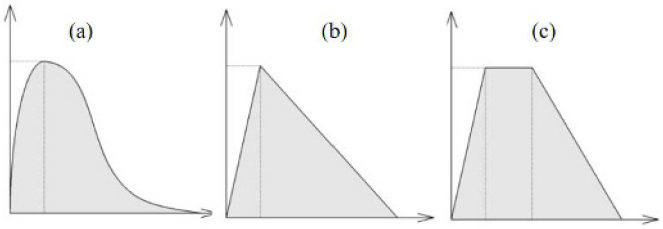

Fig. 1. Various traction separation laws: (a) exponential; (b) bilinear. (c) trapezoidal.

3 Sandwich structural mechanics model

The used sandwich structure is composed of two components, i.e. glass fiber composite plate (GFRP), aramid honeycomb structure (AHCS), which are joined together by glue ply, as demonstrated in Fig. 2.

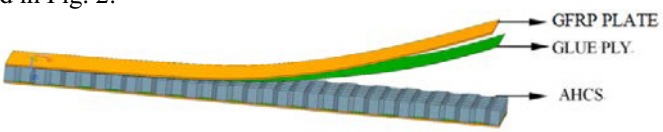

Fig. 2. Schematic diagram of the used sandwich structure.

3.1 The peel strength of the sandwich structure

When two materials with different stiffness are bonded together to form a structure, the structure specimen is subjected to the action of opening the bonding surface, called peeling.

A 90° float roll stripping method is used to test the peel strength of the sandwich structure. Since the force reception surface of the bonding surface is a straight line during the load application, the peel strength test is independent of the bonding surface area. The average peel strength can be calculated as,

$$M=(P_b-P_o)(D-d)/2b \tag{13}$$

Where M is the average peel strength, P_b and P_o are the average peel load and the resistance load, D is the diameter of the roller flange, d is the diameter of the roller and b is the width of the specimen.

3.2 The materials of the specimen

In the sandwich construction, the materials used for the panels and core are different. The panel of the specimen is GFRP and the lamina elastic constants of GFRP are listed in Table 1. On the other hand, the material of the core is aramid papers, and the properties of the aramid papers are provided in Table 2. Hansort 4301 is selected as the material of the glue joint, where the characteristics of the material are shown in Table 3.

Table 1. The lamina elastic constants of GFRP.

Lamina Elastic Constants					
E11	35(GPa)	E22	4.5(GPa)	E33	4.5(GPa)
ν12	0.35	ν13	0.35	ν23	0.45
G12	32.3(GPa)	G13	15.8(GPa)	G23	15.8(GPa)

Table 2. The properties of aramid papers.

Density t(mm3)	Compressive modulus(MPa)	Compressive Strength(MPa)	Shear modulus(MPa)	Tensile Strength(MPa)
2.9e-9	280	2.6	138	3.5

Table 3. The properties of Hansort 4301.

Gram weight(g/m2)	elasticity modulus(MPa)	Shear modulus(MPa)	Poisson ratio ν	Strength δ(MPa)	Shear Strength τ(MPa)
200±4	1000	385	0.3	6.8	25

3.3 Mechanical model and finite element model

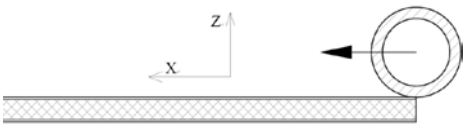

Fig. 3. Schematic diagram of the honeycomb sandwich structure in the cylinder peel strength test.

Fig. 4. Finite element of the honeycomb sandwich structure.

According to the sample size, a three-dimensional peeling model of the sandwich honeycomb roller is established. The roller model and honeycomb structure are set as shell elements, and the panel and cohesive element are solid elements for meshing, and the bonding thickness is set as 0.1mm. In order to increase the simulation accuracy, the panel, cohesive element and the honeycomb sandwich are connected in the form of a common node to establish a finite element model. This modeling method can effectively improve the simulation accuracy.

3.4 Simulation analysis of mechanical properties of the sandwich structure

A reference point constraint is established for the center of the drum with an applied angular velocity. Fig.5 is the deformation of the panel structure when peeling off, and Fig.6 is the curve of bending moment load and time to the peeling of the roller. Based on the formula F=M/D, the peeling load of the sandwich structure can be obtained, while the average peeling load of the roller is 109.71N.

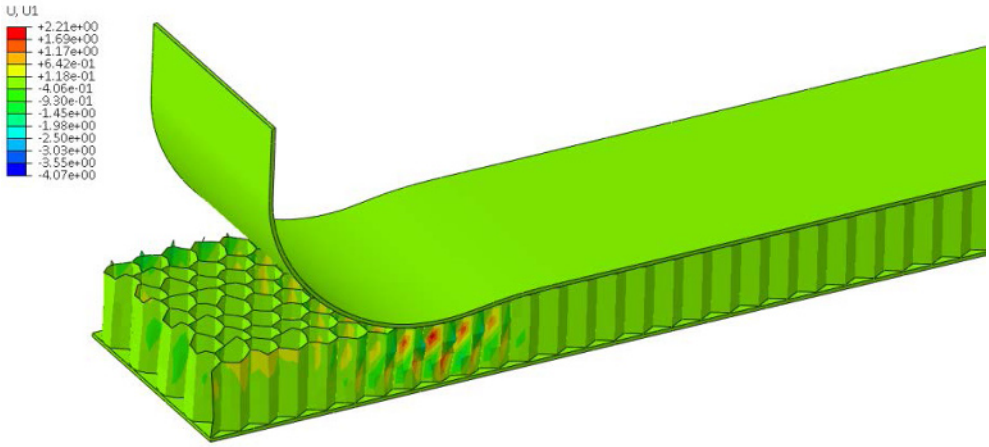

Fig. 5. Vertical deformation cloud image of the sandwich structure.

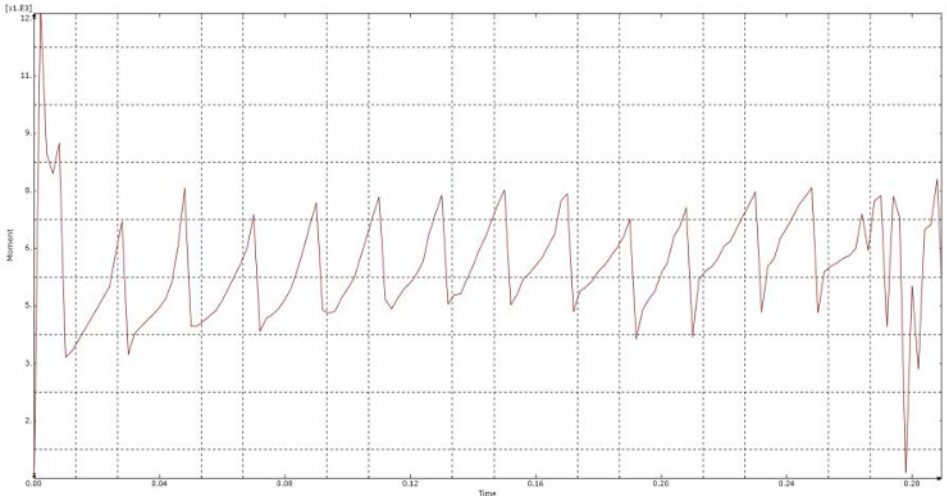

Fig. 6. Stripping bending moment curve of the sandwich structure.

3.5 Sandwich structure drum peeling experiment.

3.5.1 Specimen specification

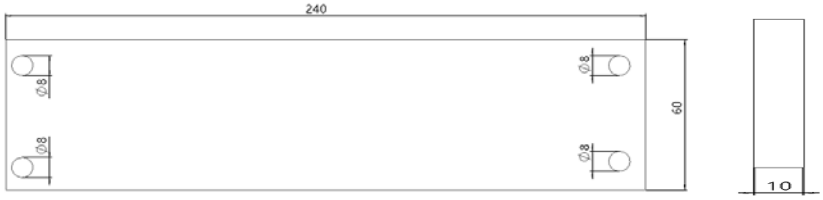

Fig. 7. Roller peeled sample.

Table 4. Specimen size.

Spline name	L(mm)	W(mm)	T(mm)
Roller peel test spline	240	60	10

3.5.2 Sample preparation

The samples are prepared in the following steps:

1.) Sampling basic data measurement and labelling;

2.) Cut off both ends of the unpeeled surface to a length of 30mm, leaving only the panel to be peeled off;

3.) Production and Pasting of Wood Reinforcement Sheet (Cured at 90℃);

4.) Punching (punch holes at the joint with the drum, the center distance of the holes is 45mm with mechanical punches);

5.) Scribe (150-180mm) peeling end point.

A flanged cylinder is used to measure the peel strength of the panel and the core from the glass panel in the sandwich structure. The panel is connected to the cylinder at one end, and the furniture at the other end, the flange is connected to the loading belt, and the tensile loading belt is connected. When the cylinder rolls upwards to peel off the panel from the sandwich structure, the loading belt on the flange is different from the panel on the cylinder with certain distance. The peel strength of the sandwich structure roller is actually the resistance per unit width of the separation between the panel and the core, where the loading speed is (20-30) mm/min.

3.5.3 Experimental result and analysis

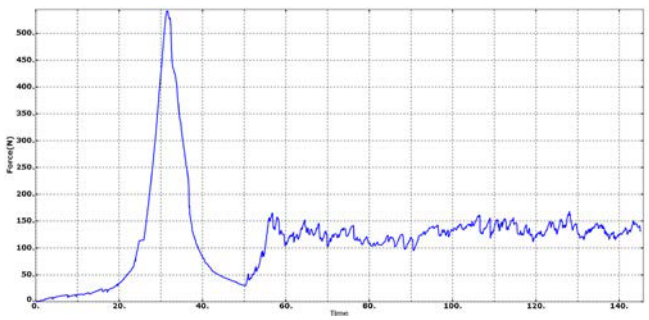

Fig. 8. Roller peeling sample test curve (The average load of the curve is taken in the middle of 60-140S).

We select the appropriate range and use MATLAB to calculate the average peel load.

Table 5. Sample test result.

Number	Average Load/N
1	112.83
2	128.75
3	125.75

Fig. 9. Roller peeling sample test.

4 Conclusion

This paper studies the strength analysis via CMZs with light-weight structure materials. During the tests, the average peeling load of the simulation is 109.71N, the average peeling load of the test is 122.44N, and the error is about 10% in such sandwich structure. The accuracy of the simulation model is verified by the comparison between the simulation results and the actual experimental load values. The CMZ model can be used to verify that the interlayer bonding model can be used to predict the occurrence and expansion of damage to the interlayer unit of the composite materials.

This work is supported by Tianjin “The Belt and Road Initiative” technical R & D cooperation and industrialization projects (19YDYGHZ00070).

References

1. Fowler, J. W. Grand Challenges in Modeling and Simulation of Complex Manufacturing Systems [J]. Simulation Transactions of the Society for Modeling & Simulation International, 2015, 80(9):469-476.
2. Mourtzis, D., M. Doukas, and D. Bernidaki. "Simulation in Manufacturing: Review and Challenges." Procedia Cirp 25(2014):213-229.
3. Ansari, M. Z., et al. "Compressive Behaviour of Polymer/Honeycomb Sandwich Composites." Advanced Materials Research 278.4(2015):283-288.
4. Rao, S., K. Jayaraman, and D B hattacharyya. "Short fibre reinforced cores and their sandwich panels: Processing and evaluation." Composites Part A Applied Science & Manufacturing 42.9(2011):1236-1246.

5. Zhang, S., et al. "Theoretical analysis of high strength and anti-buckling of three-dimensional carbon honeycombs under shear loading." Composites Part B Engineering 219.5067(2021):108967.
6. YAVARI, and ARASH. "Generalization of Barenblatt's cohesive fracture theory for fractal cracks." Fractals-complex Geometry Patterns & Scaling in Nature & Society 10.02(2002):189-198.
7. Park, K., and G. H. Paulino. "Cohesive Zone Models: A Critical Review of Traction-Separation Relationships Across Fracture Surfaces." Applied Mechanics Reviews 64.6(2015):1002.
8. Spring, D. W., and G. H. Paulino. "A growing library of three-dimensional cohesive elements for use in ABAQUS." Engineering Fracture Mechanics 126(2014):190-216.
9. Teimouri, F., M. Heidari-Rarani, and F. H. Aboutalebi. "Finite element modeling of mode I fatigue delamination growth in composites under large-scale fiber bridging." Composite Structures (2021):113716.
10. Zhang, J., et al. "Effect of the Cohesive Law Shape on the Modelling of Adhesive Joints Bonded with Brittle and Ductile Adhesives." International Journal of Adhesion & Adhesives 85(2018):37-43.